Jul 1st, 12:00 AM

Numerical Simulation of Flow Patterns and Mass Exchange Processes in Dead Zones

C. Gualtieri

iEMSs 2008: International Congress on Environmental Modelling and Software
Integrating Sciences and Information Technology for Environmental Assessment and Decision Making
4th Biennial Meeting of iEMSs, http://www.iemss.org/iemss2008/index.php?n=Main.Proceedings
M. Sànchez-Marrè, J. Béjar, J. Comas, A. Rizzoli and G. Guariso (Eds.)
International Environmental Modelling and Software Society (iEMSs), 2008

Numerical Simulation of Flow Patterns and Mass Exchange Processes in Dead Zones

C. Gualtieri

Department of Hydraulic, Geotechnical and Environmental Engineering (DIGA), University of Napoli Federico II, Napoli, Italy (carlo.gualtieri@unina.it)

Abstract: Contaminants and nutrients transport in streams and rivers is significantly affected by the presence of dead zones that are due to geometrical irregularities, that may have both natural and anthropic origins. Dead zones are characterized by mean flow velocity in the main stream direction approximately equal to zero and by exchange processes of solutes with the main stream. This paper presents the preliminary results of a numerical study undertaken to investigate the fundamental flow phenomena around and inside a simplified geometry, representative of flow in natural rivers with dead zones. Exchange rates between the dead zone and the channel were calculated resulting in a good agreement with previous literature experimental values for the same geometry.

Keywords: Environmental Fluid Mechanics; Numerical Simulation; Mass exchange; Dead zones; Verification.

1. INTRODUCTION

Solute transport in streams and rivers is strongly related to river characteristics, such as mean flow velocity, velocity distribution, secondary currents and turbulence features. These parameters are mainly determined by the river morphology and the discharge conditions. Most natural channels are characterized by relevant diversity of morphological conditions. In natural channels, changing river width, curvature, bed form, bed material and vegetation are the reason for this diversity, whereas in rivers which are regulated by man-made constructions, such as spur dikes, groins, stabilized bed and so on, the morphological diversity is often less pronounced and, thus, flow velocities are more homogeneous. In natural channels, some of these morphological irregularities, such as small cavities existing in sand or gravel beds, side arms and embayments, can produce recirculating flows which occur on different scales on both the riverbanks and the riverbed. These irregularities act as dead zones for the current flowing in the main stream direction. In regulated rivers, groyne fields are the most important sort of dead zones. Groyne fields can cover large parts of the river significantly affecting its flow field. Dead-water zones or *dead zones* can be defined as geometrical irregularities existing at the river periphery, within which the mean flow velocity in the main stream direction is approximately equal to zero [Weitbrecht 2004]. Dead zones significantly modify velocity profiles in the main channel as well affect dispersive mass transport within the river. Thus, in recent years exchange processes between the main stream and its dead zones were increasingly studied, mostly using experimental laboratory and field works [Kimura and Hosoda, 1997; Wallast et al., 1999; Uijttewaal, 1999; Muto et al., 2000a; Muto et al., 2000b; Weitbrecht and Jirka, 2001a; Weitbrecht and Jirka, 2001b; Uijttewaal et al., 2001; Kurzke et al., 2002; Engelhardt et al., 2004; Uijttewaal, 2005; Brevis et al., 2006; Le Coz et al., 2006; Jamieson and Gaskin, 2007; Weitbrecht et al., 2008]. Also, numerical studies were recently carried out to investigate flow hydrodynamics in channels with groyne fields [McCoy et al., 2008].

The objective of this paper is to present the preliminary results of a numerical study undertaken to investigate the fundamental flow phenomena around and inside a simplified

geometry, representative of flow in natural rivers with dead zones. Also, exchange processes of a solute between the main flow and the dead zones were studied with the evaluation of the exchange coefficient between the main flow and the dead zones. For the present study, two-dimensional steady-state numerical simulations were performed with Multiphysics 3.3™ in three different geometries representing dead zones, that is a single rectangular embayment and a groyne field with 10 and 5 groynes, respectively. These geometries were those previously experimentally studied by Muto et al. [2000a; 2000b], Wallast et al. [1999], and Weitbrecht and Jirka [2001b].

2. LITERATURE REVIEW

As already outlined, in streams and rivers, mass transport of solutes is significantly affected by the exchange processes between the main flow in the channel and the dead-water zones existing at its periphery [Valentine and Wood, 1977; Weitbrecht 2004]. In natural channels, dead zones can be formed by sand or gravel banks, side cavities, small pockets at the river bed or any other irregularity in the morphology both at the riverbanks and at the riverbed, whereas in regulated rivers, spur dikes and groin fields are typical dead zones. Due to momentum exchange across the interface with the main channel, flow patterns inside the dead zones are characterized by recirculating flows which occur on different scales and exhibit flow velocity in the main stream direction close to zero. Therefore, the most important effect of dead zones on mass transport in rivers is the storage of some amount of the contaminants or nutrients being transported by the main stream inside the dead zones, that is some mass of solutes are first trapped in the dead zones and only later, after an average storage time T_D, are released back into the main flow. The storage time depends on the strength of the exchange processes occurring between the main stream and the dead zones, which are due mostly to turbulent mixing in the lateral or in the vertical direction, if the dead zone is at the riverbanks or at the riverbed, respectively [Muto et al., 2000b; Weitbrecht, 2004]. As discussed below in details, the flow structure in a dead zone consists of a mixing layer, a primary eddy and a core region within this eddy. Depending on the dead zone aspect ratio a smaller corner eddy may exist. Turbulent mixing around a dead zone is mostly governed by two-dimensional coherent structures in the mixing layer between the dead zone and the main channel, even if other mechanisms and 3D structures are believed to be also involved [Brevis et al., 2006; Le Coz et al., 2006; Jamieson and Gaskin, 2007]. The effect of these exchange processes on the transport of solutes in a river with dead zones can be quantified considering the average transport velocity of solutes, defined as the velocity of the center of mass of the tracer cloud, and the strength of the longitudinal dispersion process, which describes the rate of stretching of the tracer cloud [Weitbrecht, 2004].

In a channel without dead zones, the average transport velocity of a tracer cloud that is completely mixed over the river cross-section equals the mean flow velocity. If dead zones are present, the part of the tracer cloud trapped in the dead zones is retarded compared to the part of tracer cloud travelling in the main stream with the mean flow velocity. In this case, the transport velocity of the tracer cloud is lower than the mean flow velocity.

Also, dead zones produce an increased stretching of a passing tracer cloud, which means that the longitudinal dispersion is enhanced. This results in a tail of the contaminants cloud longer than that predicted by the 1-D advection-diffusion equation [Valentine and Wood, 1979, Czernuszenko et al., 1998] and the length of the tail depends on the exchange between the main flow and the dead zones. This could be explained by two processes [Weitbrecht, 2004]. First, dead zones modify the transverse profile of flow velocity in the main channel and increase lateral turbulent mixing, which are the determining parameters for longitudinal dispersion (Fig.1). It is well known that transverse mixing is important in determining the rate of longitudinal mixing because it tends to control the exchange between regions of different longitudinal velocity. Particularly, transverse mixing and longitudinal mixing are inversely proportional. A strong transverse mixing tends to erase the effect of differential longitudinal advection and pollutants particles migrate across the velocity profile so fast that they essentially all move at the mean speed of the flow, causing

only a weak longitudinal spreading. On the other hand, a weak transverse mixing implies a long time for differential advection to take effect, so the pollutants patch is highly distorted while it diffuses moderately in the transverse direction and longitudinal mixing is large (Cushman-Roisin, 2007). Second, tracer cloud is stretched because solute parcels are trapped within the dead zones and only later released back into the main channel. Both processes result in an enhanced longitudinal dispersion, which leads to lower peak levels but to a longer period during which critical values could be exceeded. Finally, these processes are strongly related to the geomorphological conditions of the dead zones.

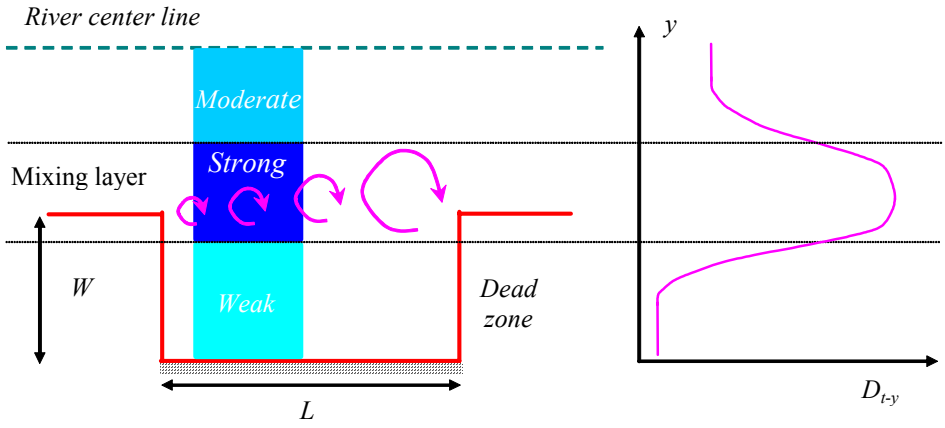

Figure 1. Transverse turbulent diffusivity profile in a river with dead zone

Since classical 1-D advection-diffusion equation cannot satisfactorily describe observed tracer concentrations from an instantaneous release in natural channels, where there is a relevant amount of dead zones, models accounting for the dead zones effects were proposed. The basic idea of the dead-zone model (DZM) is to distinct within the cross-section of a river, two zones, the main stream and the dead-zone. In the main stream the mass transport is governed by advection in the longitudinal direction, longitudinal shear due to the velocity distribution and transverse turbulent diffusion. Thus, in the main stream transport processes can be modeled under well mixed conditions using 1-D advection-diffusion equation. In the dead zone, since velocity in the main stream direction is close to zero, transverse turbulent diffusion across the interface between the dead zone and the main stream is the dominant mechanism, which leads to momentum and mass exchange processes. Assuming that in the dead zone the solute concentration is uniform, mass exchange between the dead zone and the main stream is proportional to the difference of the averaged concentration in the dead zone and in the main channel. To set up the DZM, conservation of mass for the main stream and the dead-zone has to be considered, that is [Czernuszenko et al., 1998; Weitbrecht, 2004; Weitbrecht et al., 2008]:

$$\frac{\partial C_S}{\partial t} = -U\frac{\partial C_S}{\partial x} + D_L\frac{\partial^2 C_S}{\partial x^2} + \frac{h_E\, E}{h_S\, B}\left(C_D - C_S\right) \tag{1a}$$

$$\frac{\partial C_D}{\partial t} = -\frac{h_E\, E}{h_D\, W}\left(C_D - C_S\right) \tag{2a}$$

where C_S and C_D are the solute concentration in the main stream and in the dead zone, respectively, U is mean velocity, D_L is longitudinal dispersion coefficient, B and W are channel width and dead zone width, respectively, h_S, h_D and h_E are the water depth in the main channel, in the dead zone and at their interface, respectively, and E is the exchange velocity across this interface (Fig.1). Usually, the ratios $h_E E/h_S B$ and $h_E E/h_D W$ which have the unit of [T^{-1}], are called *exchange coefficients* K_S and K_D and the above equations yield:

$$\frac{\partial C_S}{\partial t} = -U\frac{\partial C_S}{\partial x} + D_L\frac{\partial^2 C_S}{\partial x^2} + K_S\left(C_D - C_S\right) \tag{1b}$$

$$\frac{\partial C_D}{\partial t} = -K_D \left(C_D - C_S \right) \tag{2b}$$

As previously noted, one important parameter of the dead zone is its *average storage time* T_D, which could be approximated by calculating the time needed to completely change the water volume in the dead zone. Thus, T_D could be obtained dividing the dead zone volume by the exchange velocity and the interface area, if L is the dead zone length, as [Weitbrecht, 2004]:

$$T_D = \frac{W\, L\, h_D}{E\, L\, h_E} = \frac{1}{K_D} \tag{3}$$

which demonstrates that T_D and K_D are reciprocal, that is higher exchange coefficients correspond to lower retention time inside the dead zone. Notably, if the concentration in the main stream is zero, Eq.(2b) corresponds to first-order decay law. Thus, for the case of a instantaneous and homogeneous mass release into the dead zone, the change of concentration inside the dead zone is described by:

$$C_D(t) = C_0\, exp\left(-K_D\, t\right) = C_0\, exp\left(-t/T_D\right) \tag{4}$$

where C_0 is the initial concentration in the dead zone. Eq.(4) confirms that the exchange coefficient K_D represents the slope of the decay process occurring inside the dead zone. Usually, K_D is normalized with the mean velocity in the mean stream and the width of the dead zone giving a dimensionless exchange coefficient [Valentine and Wood, 1979]:

$$k = \frac{K_D\, W}{U} \tag{5a}$$

Note that if the water depth in the main stream and in the dead zone are equal, that is h_E=h_D, the exchange coefficient K_D becomes:

$$K_D = \frac{E}{W} \tag{6}$$

and k is the ratio between the exchange velocity and the main stream velocity:

$$k = \frac{E}{U} \tag{5b}$$

Typical values of k parameter are in the range from 0.012 to 0.05 [Valentine and Wood, 1979; Wallast et al., 1999; Muto et al., 2000b; Weitbrecht and Jirka, 2001b; Weitbrecht, 2004].

Dimensional analysis leads to conclude that dimensionless exchange coefficient k has the form [Weitbrecht, 2004]:

$$k = f\left(Re, Fr, Pe, \frac{k_s}{h_S}, \frac{h_D}{h_S}, \frac{B}{h_S}, \frac{W}{L}, \alpha, S \right) \tag{7a}$$

where Re, Fr and Pe are Reynolds, Froude and Peclet number, respectively, k_s is bed roughness and α and S are the inclination to the main flow direction and the shape of the dead zone. However, it can be stated that under typical turbulent flow and low Froude number conditions, a major influence on the mass exchange is given by the aspect ratio of the dead zone W/L and the inclination angle leading to discard most of the parameters involved in eq.(7a), which yields:

$$k = f\left(\frac{W}{L}, \alpha \right) \tag{7b}$$

Previous experimental studies demonstrated that the dimensionless exchange coefficient k decreased with the increasing aspect ratio W/L of the dead zone [Muto et al., 2000a, 2000b; Uijttewaal et al., 2001; Weitbrecht and Jirka, 2001a; Weitbrecht et al., 2008].

Literature studies have already pointed out some typical patterns of flow structure around and inside a dead zone which are depending on the aspect ratio W/L [Booij, 1989; Kimura and Hosoda, 1997; Uijttewaal, 1999; Muto et al., 2000b; Uijttewaal et al., 2001; Brevis et al., 2006; Jamieson and Gaskin, 2007]. The flow inside a dead zone is a type of shear-driven cavity flow [Shen and Floryan, 1985; Shankar and Deshpande, 2000], where the flow separates at the upstream corner of the cavity and forms a wake, like behind a backward facing step, in the lee of the upstream end of the cavity. In turbulent flow, the wake may be bounded by a plane mixing layer (ML), which is the shear flow formed in the region between two co-flowing streams of different velocities [Raupach et al., 1996]. Due to the velocity difference, this region is characterized by a strong inflection in the mean velocity profile which gives rise to hydrodynamic instability processes resulting in the development of the mixing layer. Large scale turbulent structures with the vorticity aligned with the main flow vorticity are continuously fed from the main flow. These structures determine a turbulence length scale in the order of the width of the mixing layer, which develops in self-preserving way with a constant spreading rate, depending only on the relative velocity difference across the mixing layer [Booij and Tukker, 2001]. Depending on the dead zone aspect ratio, this wake may entirely fill the dead zone as a primary eddy, but for low aspect ratio, secondary or more eddies start to develop. All those eddies are mainly driven by the main stream flow. Particularly, if the aspect ratio *W/L* is in the range from 0.5 to 1.5 only the primary recirculating eddy is present inside the dead zone and it covers almost the complete area of the dead zone. If *W/L<0.5*, a second eddy develops in the upstream corner of the dead zone. This secondary gyre has no direct contact with the main stream so it is driven by momentum exchange with the primary eddy. Thus, flow velocity in this area is quite slow. With even smaller aspect ratio, that is *W/L<0.2*, the two eddies remain but the main flow starts to penetrate into the dead zone [Uijttewaal, 1999]. On the other hand, if *W/L>1.5*, a second eddy develops behind the primary in transverse direction to the main stream.

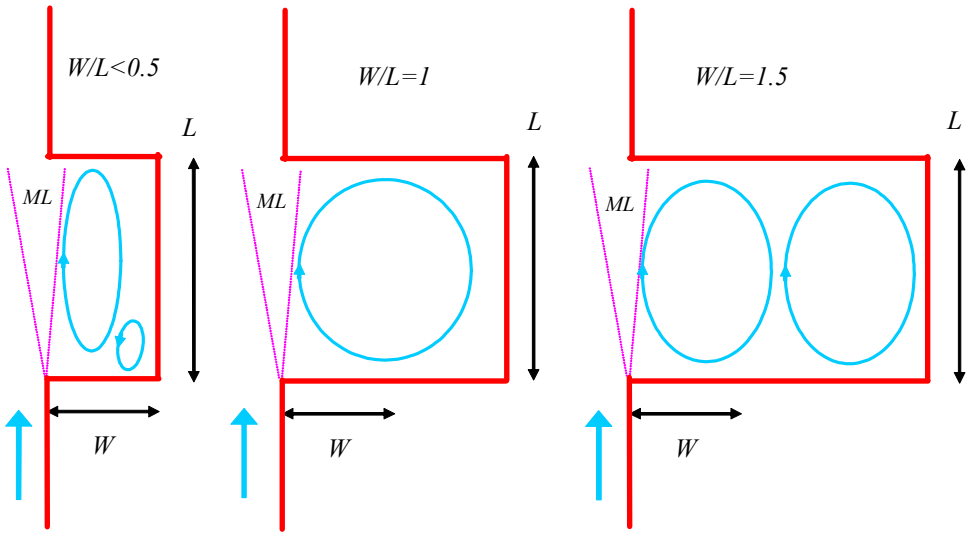

Figure 2. Influence of aspect ratio W/L in flow field in a dead zone

Experimental observations with Particle Image Velocimetry (PIV), Laser Induced Fluorescence (LIF) and dye methods of flow dynamics confirmed that large-scale coherent structures were generated at the head of the upstream wall of the dead zone and were growing as they were advected within the mixing layer governing mass exchange across the interface between the dead zone and the main stream [Uijttewaal et al., 2001; Weitbrecht and Jirka, 2001b; Jamieson and Gaskin, 2007]. Since a river can be considered to have shallow flow, that is horizontal length scale dominates on vertical length scale, these coherent structures are expected to be mainly two-dimensional. However, some experimental studies pointed out that the exchange process is not uniform over the water depth and the exchange rate increases towards the water surface [Weitbrecht and Jirka,

2001a; Brevis et al., 2006], whereas intermittent vertical structures were observed [Jamieson and Gaskin, 2007]. Recent experimental studies addressed the role in the exchange process of Kelvin-Helmholtz instabilities occurring at the dead zone-main stream interface [Brevis et al., 2006].

Coming back to the dimensionless exchange coefficient k, it was recognized in some laboratory experimental works that in dead zone with $W/L<0.5$ the exchange between the dead zone and the main stream was a two stage process, where two different time scales could be observed [Booij, 1989; Uijttewaal et al., 2001; Engelhardt et al., 2004; Jamieson and Gaskin, 2007]. Some authors ascribed this two stage structure to an initial, fast exchange between the primary eddy and the main stream followed by an exchange between the primary eddy and the smaller, secondary eddy in the upstream corner of the dead zone [Booij, 1989; Uijttewaak et al., 2001]. Other authors suggested a model with a fast exchange for the mixing layer and a slower exchange between the primary eddy and its relatively standing core [Engelhardt et al., 2004; Jamieson and Gaskin, 2007].

3. NUMERICAL SIMULATIONS

As above outlined, the exchange process between a dead zone and the main stream is mainly governed by two-dimensional large-scale coherent structures and flow structure inside and around the dead zone may be considered as two-dimensional [Muto et al., 2000a; Uijttewaal et al., 2001; Weibrecht, 2004]. Thus, two-dimensional or depth-averaged models may be applied to describe hydrodynamics and mass-transfer processes. These computational fluid dynamics (CFD) models are based on the mass conservation equation and the Navier-Stokes equations of motion. Since the flow in the tank is turbulent, these equations must be averaged over a small time increment applying Reynolds decomposition, which results in the Reynolds-averaged Navier-Stokes equations (RANS). For a planar, incompressible flow these equations are:

$$\frac{\partial \overline{u}}{\partial x}+\frac{\partial \overline{v}}{\partial y}=0 \tag{8}$$

$$\begin{aligned}\overline{\rho}\left(\frac{\partial \overline{u}}{\partial t}+\overline{u}\frac{\partial \overline{u}}{\partial x}+\overline{v}\frac{\partial \overline{u}}{\partial y}\right)&=\overline{\rho}\,g_x-\frac{\partial \overline{p}}{\partial x}+\left(\mu+\rho\,\nu_t\right)\nabla^2\overline{u}\\ \overline{\rho}\left(\frac{\partial \overline{v}}{\partial t}+\overline{u}\frac{\partial \overline{v}}{\partial x}+\overline{v}\frac{\partial \overline{v}}{\partial y}\right)&=\overline{\rho}\,g_y-\frac{\partial \overline{p}}{\partial y}+\left(\mu+\rho\,\nu_t\right)\nabla^2\overline{v}\end{aligned} \tag{9}$$

where ρ and μ are fluid density and viscosity, p is fluid pressure and u, v are velocity components in the x and y directions, respectively. The overbar indicates time-averaged quantities. Notably, in eq. (9) there is the turbulent kinematic viscosity ν_t, that if isotropic turbulence assumption holds could be estimated following the k-ε model approach as:

$$\nu_t=\frac{C_\mu\,k'^2}{\varepsilon'} \tag{10}$$

where k' and ε' are turbulent kinetic energy per mass unit and its dissipation rate, respectively, and $C_\mu=0.09$. These parameters are estimated with the classical two equations of k-ε model:

$$\underbrace{\frac{\partial k'}{\partial t}}_{\text{Change in } k'}+\overline{\overline{V}}\cdot\nabla k'=\underbrace{\frac{\nu_t}{\sigma_k}\nabla k'}_{\text{Flux}}-\underbrace{\varepsilon'}_{\text{Dissipation}}+\underbrace{2\,\nu_t\,\overline{\overline{D}}\,\overline{\overline{D}}}_{\text{Production}} \tag{11}$$

$$\frac{\partial \varepsilon'}{\partial t}+\nabla\cdot\varepsilon'\overline{\overline{V}}=\frac{\nu_t}{\sigma_\varepsilon}\nabla\varepsilon'+2\,\nu_t\,C_{1\varepsilon}\frac{\varepsilon'}{k'}\overline{\overline{D}}\,\overline{\overline{D}}-C_{2\varepsilon}\frac{\varepsilon'^2}{k'} \tag{12}$$

where $\overline{\overline{D}}$ is deformation tensor, whereas C_μ, σ_k, σ_ε, $C_{1\varepsilon}$ and $C_{2\varepsilon}$ are constants, and their values are listed in Table 1.

Table 1. Values of the constants of *k-ε* model

C_μ	σ_k	σ_ε	$C_{1\varepsilon}$	$C_{2\varepsilon}$
0.09	1.00	1.60	0.1256	1.92

These equations were solved using Multiphysics 3.3™ modeling package, which is a commercial multiphysics modeling environment (Multiphysics, 2006). Multiphysics 3.3™ can solve for the same flow domain both motion equations and advection-diffusion equation. Particularly, both the *k-ε* model application mode and the advection-diffusion application mode were used. They solve eqs. from (8) to (12) for the pressure $\overline{p}$, the velocity vector components $\overline{u}$ and $\overline{v}$, and *k-ε* model parameters within the domain of the flow (Multiphysics, 2006). Multiphysics 3.3™ was applied to three different geometries representing dead zones, that is a single rectangular embayment and a groyne field with 10 and 5 groynes, respectively. These geometries were those previously experimentally studied by Muto et al. [2000a; 2000b], Wallast et al. [1999], and Weitbrecht and Jirka [2001b]. The studied geometries are presented in Fig.3.

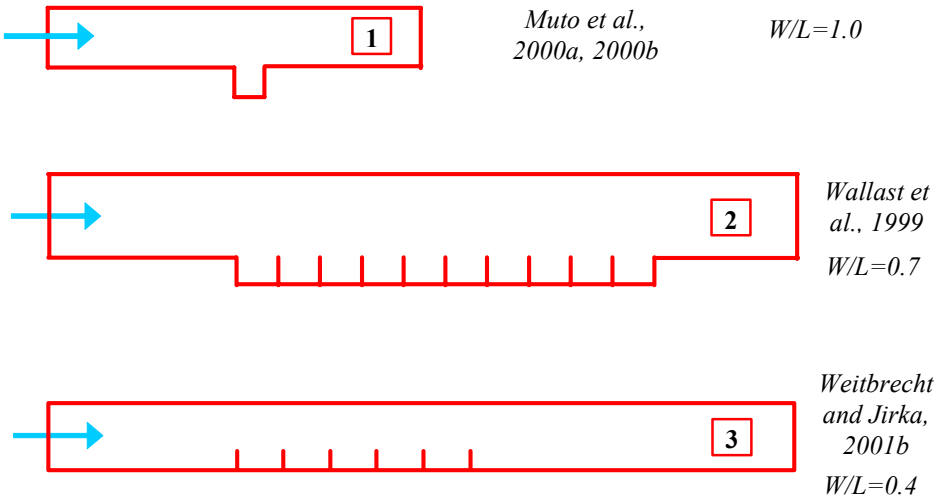

Figure 3. Dead zone geometries investigated in this study

For the simulations, *inflow* boundary condition was applied at the inlet, with uniform velocity profile and a fixed value for *k'* and *ε'* parameters, whereas *neutral* boundary condition was applied at the outlet. Finally, *logarithmic law of the wall* boundary condition was applied to the remaining boundaries, that is at walls and dead zones baffles.
Table 2 lists the main input parameters of the performed simulations.

Table 2. Characteristics of the performed simulations

Geometry	W – m	L – m	W/L	U_{in} – m/s	Reference
1	0.16	0.16	1.00	0.37	Muto et al., 2000a, 2000b
2	0.75	1.12	0.67	0.35	Wallast et al., 1999
3	0.50	1.25	0.40	0.16	Weitbrecht and Jirka, 2001b

The *k-ε* model application mode uses Lagrange *p2-p1* elements to stabilize the pressure. Thus, second order Lagrange elements model the velocity components and *k'* and *ε'* parameters while linear elements model the pressure. The default element settings in this application mode always provide one order higher Lagrange elements for the velocity components than for the pressure.

For the simulations water with density ρ=1000 Kg/m³ and molecular viscosity $\mu=1.00\cdot10^{-3}$ Kg/m×s, was selected as fluid. The mesh generation process was made assuming, among the others, as maximum element size scaling factor, element growth rate and mesh

curvature factor 1, 1.3 and 0.3, respectively. Different values for the maximum element size were selected for the main stream and the dead zone. Finer values were selected in the dead zones and in the mixing layer, where errors tend to be large due to significant velocity gradients. For geometry n.1, maximum element sizes were 0.5 and 0.05 m in the main stream and in the dead zones, respectively. For geometry n.2, maximum element sizes were 0.5 and 0.075 m in the main stream and in the dead zones, respectively, whereas a maximum element size of 0.05 m was assigned at the dead zone-main channel interface. For geometry n.3, maximum element sizes were 0.02, 0.01, 0.005 and 0.002 m in the main stream, at the channel walls, in the dead zone and at the dead zone-main channel interface, respectively. Therefore, the mesh for geometry n.1, n.2 and n.3 has 9450, 10172 and 10434 elements, respectively, with a minimum element quality of 0.7040, 0.6802, and 0.7090, respectively. The number of degrees of freedom were 101695, 109320, and 112456, respectively. About the solver settings, for steady-state analysis, stationary non-linear solver with direct linear system solver was used, where the relative tolerance and the maximum number of iterations were set to $1.0 \cdot 10^{-6}$ and 45, respectively. Streamline diffusion was introduced too.

4. ANALYSIS OF RESULTS. DISCUSSION

Numerical simulations provided field velocity and pressure, kinematic viscosity ν_t, k' and ε' values throughout the flow domain. Fig.4 presents measured (left) and simulated (right) velocity values (surface colour) and velocity vectors (arrows) in the square cavity experimentally studied by Muto et al. (2000a, 2000b), where the flow in the main stream is from the left. Inside the cavity a recirculating primary eddy was observed and its core with very low velocities (blue) is located around the midpoint of the cavity. Higher velocities can be observed in the mixing layer developing at the interface between the cavity and the main channel. Analysis of flow field demonstrated that experimental flow patterns were fairly reproduced by numerical results.

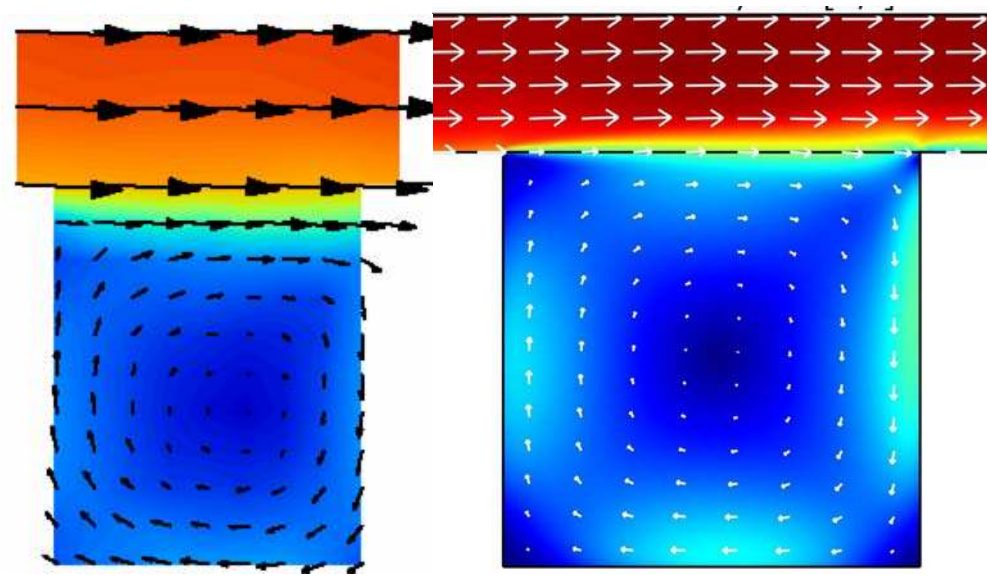

Figure 4. Measured (left) and simulated (right) velocity values and velocity vectors in the square cavity, that is geometry n.1

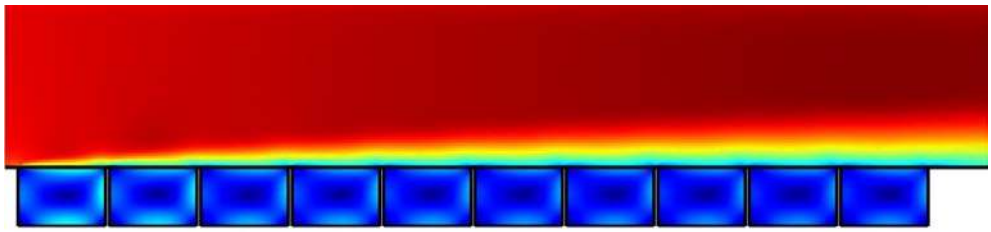

Figure 5. Simulated velocity values in geometry n.2

In the groyne field geometries, flow patterns are more complex. In the geometry studied by Wallast et al. (1999), with 10 groyne fields and a dead zone aspect ratio W/L equal to 0.7, the mixing layer develops from the upstream wall of the first groyne down to last groyne (Fig.5). Fig.6 presents the magnitude of the velocity field and velocity vectors in the main channel and in the groyne fields n.1 and n.2. A primary recirculating eddy is again observed but its relatively stagnant core is located in the downstream part of the dead zone.

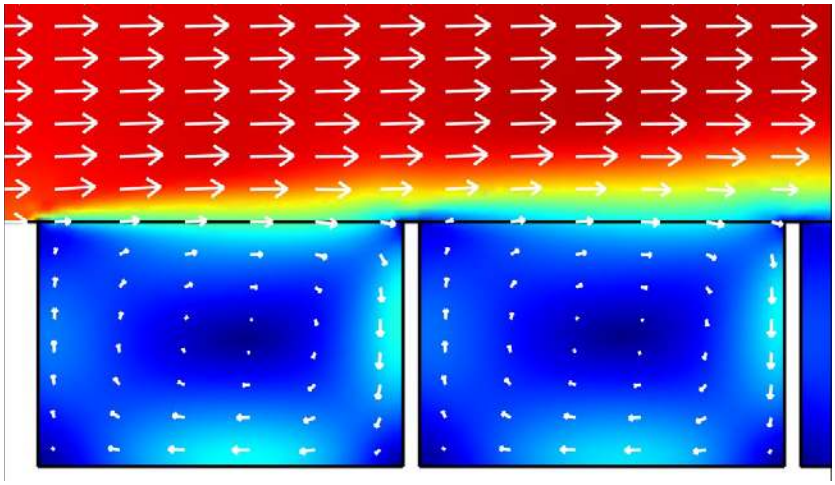

Figure 6. Simulated velocity values and velocity vectors for the groyne field n.1 and n.2

The development of the mixing layer was also observed in the geometry studied by Weitbrecht and Jirka (2001b), but in the first groyne field the primary eddy was partly located outside the dead zone due to the separation region produced by the upstream wall (Fig.7). The eddy core is located around dead zone-main channel interface. Also, the corner eddy was not observed in the numerical results.

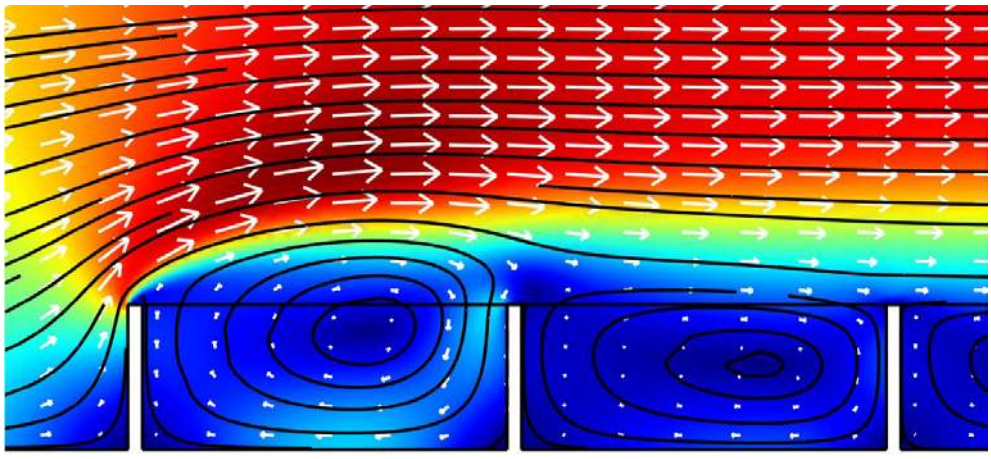

Figure 7. Simulated flow velocity values with streamlines and velocity vectors in geometry n.3

Fig.8 shows a comparison between transverse velocity along the dead zone-cross-main channel interface of the groyne field n.2 predicted by Multiphysics 3.3™ and the field data for the geometry n.3, where L is the length of the dead zone. Negative and positive values represented the exchange processes between the dead zone and the main stream highlighting a reasonable agreement between experimental data and numerical results.

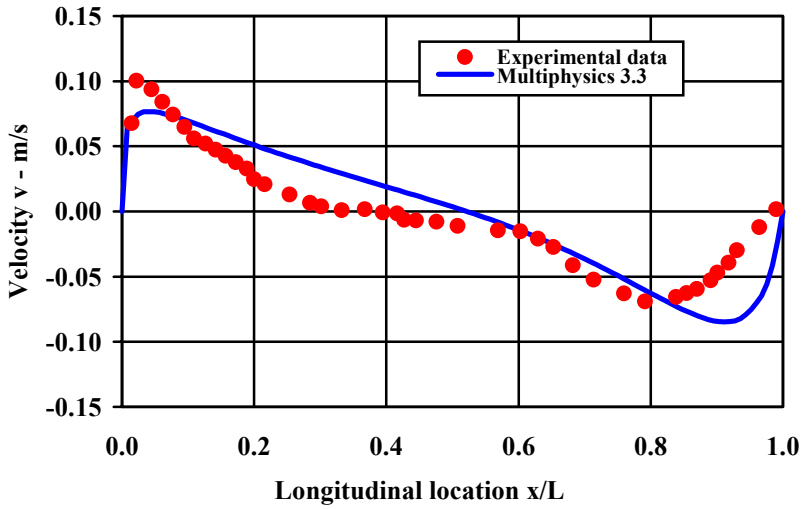

Figure 8. Transverse velocities along the dead zone-main channel interface in geometry n.3

Further comparison between experimental observations and numerical simulations was carried out using the values of dimensionless exchange coefficient k, which as above stated represents the rate of momentum and mass exchange between the dead zone and the main stream. This parameter was determined using the transverse velocity data along the dead zone-main channel interface and the procedure proposed by Weitbrecht and Jirka (2001b). That is, the norm of transverse velocity v_i was averaged over the interface, resulting in the total specific volume flux through the exchange interface. Division by 2 yielded the total specific out flux into the main channel:

$$\overline{E} = \frac{1}{2n}\sum_{i=1}^{n}|v_i| \tag{13}$$

which provides the exchange coefficient K_D and the dimensionless exchange coefficient k through (6) and (5a), respectively. For geometries n.2 and n.3, these parameters were obtained averaging their values in the 10 and 5 dead zones, respectively. Simulated k values were in the range from 0.0365 and 0.0121, which agrees with the literature available experimental data. Table 3 presents a successful comparison between numerical results and experimental data for k parameter.

Table 2. Characteristics of the performed simulations

		Multiphysics	Experiments	Reference
Geometry	W/L	k	k	
1	1.00	0.0121	0.0116	Muto et al., 2000a, 2000b
2	0.67	0.0160	0.0150	Wallast et al., 1999
3	0.40	0.0365	0.0340	Weitbrecht and Jirka, 2001b

As above noted, literature experimental data demonstrated that dimensionless exchange coefficient decreased with the increasing aspect ratio W/L of the dead zone [Muto et al., 2000a, 2000b; Uijttewaal et al., 2001; Weitbrecht and Jirka, 2001a; Weitbrecht et al.,

2008]. Thus, numerical values were plotted against the aspect ratio *W/L* and compared with the corresponding experimental data (Fig.9). Overall, numerical results were in good agreement with the experimental values and confirmed the trend with *W/L* already observed in previous literature studies.

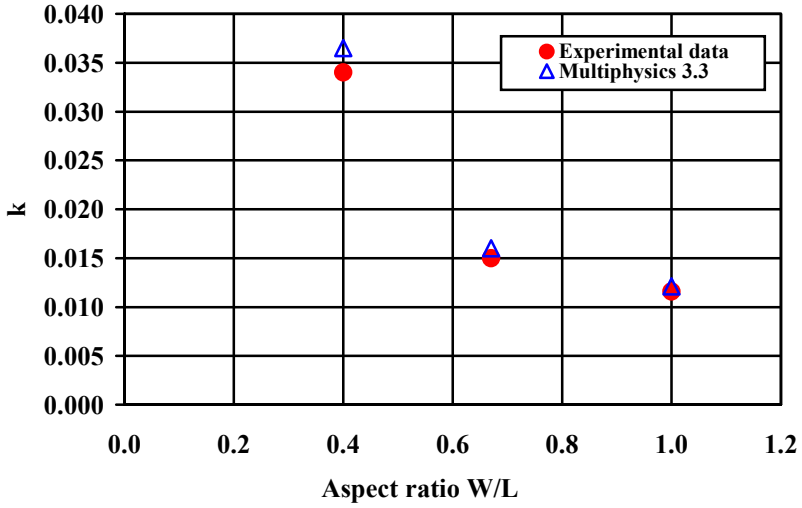

Figure 9. Dimensionless exchange coefficient *k* vs dead zone aspect ratio *W/L*

5. CONCLUSIVE REMARKS

The presence of dead zones in streams and rivers significantly affect the characteristics of mass transport. In a river, dead zones can be due to geometrical irregularities in the riverbanks and the riverbed and/or to spur dikes and groyne fields and they produce a difference between the concentration curves measured and modeled by the classical 1D advection-diffusion equation with sharper front and longer tails. In a dead zone, the mean flow velocity in the main stream direction is essentially zero and the main transport mechanism is transverse turbulent diffusion which controls the exchange processes of solutes with the main stream.

This paper presented some preliminary results of a numerical 2D study undertaken to investigate the fundamental flow phenomena around and inside a simplified geometry, representative of flow in natural rivers with dead zones. Flow patterns and exchange rates between the dead zone and the channel were simulated resulting in a good agreement with previous literature experimental values for the same geometry. The considered geometries were those experimentally studied by Muto et al. [2000a, 2000b], Wallast et al. [1999], and Weitbrecht and Jirka [2001b]. Future research will be addressed to simulate concentration field in a dead zone and to investigate the effect of the inclination of the dead zone to the main flow direction on the exchange processes.

REFERENCES

Booij, R., and Tukker. J., Integral model of shallow mixing layers, *Journal of Hydraulic Research, 39 (2)*, 169-179, 2001

Brevis, W., Niño, Y., and Vargas, J., Experimental characterization and visualization of mass exchange process in dead zones in rivers, *Proceedings of 3rd International Conference on Fluvial Hydraulics (RiverFlow 2006)*, 235-242, 2006

Cushman-Roisin, B. (2007). Environmental fate and transport, Lecture Notes, Thayer School of Engineering, Dartmouth College, NH, USA

Czernuszenko, W., Rowiński, P.M., and Sukhodolov, A., Experimental and numerical

validation of the dead-zone model for longitudinal dispersion in rivers, *Journal of Hydraulic Research, 36 (2)*, 269-280, 1998

Le Coz, J., Brevis, W., Niño, Y., Paquier, A., and Riviére, N., Open-channel side-cavities: A comparison of field and flume experiments, *Proceedings of 3rd International Conference on Fluvial Hydraulics (RiverFlow 2006)*, 235-242, 2006

Jamieson, E., and Gaskin, S.J., Laboratory study of 3 dimensional characteristics of recirculating flow in a river embayment, *Proceedings of the XXXII IAHR Congress*, 2007

Kurzke, M., Weitbrecht V., and Jirka G.H.J., Laboratory concentration measurements for determination of mass exchange between groin fields and main stream. *Proceedings of 1st International Conference on Fluvial Hydraulics River Flow 2002*, vol.1, 369-376, 2002

Multiphysics 3.3 *User's Guide*, ComSol AB. Sweden, 2007

Muto, Y., Imamoto, H., and Ishigaki, T., Velocity measurements in a straight open channel with a rectangular embayment. *Proceedings of the 12th APD-IAHR, Bangkok, Thailand*, 2000

Raupach. M.R., Finnigan, J.J., and Brunet, Y., Coherent eddies and turbulence in vegetation canopies: the mixing-layer analogy, *Boundary-Layer Meteorology, (78)*, 351-382, 1996

Shankar, P.N., and Deshpande, M.D., Fluid mechanics in the driven cavity, *Annual Review in Fluid Mechanics*, vol.32, 93-136, 2000

Shen, C., and Floryan, J.M., Low Reynolds number flow over cavities, *Physics of Fluids A*, Vol.28, n.11, November 1985, 3191-3202

Uijttewaal, W.S.J., Lehmann, D., and Mazijk, A. van, Exchange processes between a river and its groyne fields: model experiments, *Journal of Hydraulic Engineering*, *ASCE, 127 (11*), 928-936, 2001

Uijttewaal, W.S.J., Effects of groyne layout on the flow in groyne fields: laboratory experiments, *Journal of Hydraulic Engineering*, *ASCE, 131 (9)*, 782-791, 2005.

Valentine, E.M., and Wood, I.R., Longitudinal dispersion with dead zones, *Journal of Hydraulics Division, ASCE, 103 (9)*, 975-990, 1977

Valentine E.M., and Wood I.R., Experiments in longitudinal dispersion with dead zones, *Journal of Hydraulics Division, ASCE, 105 (8)*, 999-1016, 1979

Wallast, I., Uijttewaal, W., and Mazijk, A. van, Exchange processes between groyne field and main stream. *Proceedings of the XXVIII IAHR Congress*, 1999

Weitbrecht, V., and Jirka, G.H.J., Flow patterns and exchange processes in dead zones of rivers, *Proceedings of the XXIX IAHR Congress*, 2001a

Weitbrecht, V., and Jirka, G.H.J., Flow patterns in dead zones of rivers and their effect on exchange processes, *Proceedings of the 2001 International Symposium on Environmental Hydraulics*, 2001b

Weitbrecht, V., Influence of dead-water zones on the dispersive mass-transport in rivers, *Dissertation*, 2004